Fibers and Polymers (2023) 24:1799–1810
https://doi.org/10.1007/s12221-023-00157-0

Online ISSN 1875-0052
Print ISSN 1229-9197

REGULAR ARTICLE

Moisture Absorption and Tensile Behaviour of Hybrid Carbon/Flax Composites

M. Johar[1] · W. W. F. Chong[2,3] · K. J. Wong[4]

Received: 14 September 2022 / Revised: 10 February 2023 / Accepted: 19 February 2023 / Published online: 20 March 2023

Abstract

Due to environmental concerns, natural fibres are getting their importance as reinforcement in polymer composites. Nevertheless, their hydrophilic nature makes natural fibre composites susceptible to moisture attack. In this regard, one possible solution is to utilise hybrid synthetic/natural fibre composites. This paper aims to characterise the moisture absorption behaviour of carbon, flax, and hybrid carbon/flax composites. The composites were submerged in distilled water at 60 °C until saturation. Subsequently, tensile tests were conducted on dry and wet specimens. Results revealed that the moisture absorption with flax as the outer layers had attained a maximum moisture content of at least 470% higher than carbon as the outer layers. In addition, moisture absorption significantly influences the flax fibre composite, where only 27% of the specific tensile modulus was retained while the specific failure strain was doubled. The modified Halpin–Tsai equation also suggests that carbon fibre has a minimum of 5- and 3-fold larger stress transfer efficiency over the flax fibre with respect to the specific tensile modulus and strength, respectively. Through the modified Chokshi-Chaudhary-Gohil equation, the interphase volume fraction was estimated to be 8–11% for the hybrid composites. The results from this study suggest that it is better to place carbon fibre as the outer layer for hybrid carbon/flax composites to be used in outdoor applications.

Keywords Hybrid carbon/flax composites · Moisture absorption · Non-Fickian · Tensile properties · Modified Halpin–Tsai · Modified Chokshi–Chaudhary–Gohil

1 Introduction

Due to environmental concerns, natural fibres have been employed as a substitution for synthetic fibres in polymer composites. Flax fibre is one of the most popular natural fibres due to its attractive physical nd mechanical properties. Its density is lower than synthetic fibres such as carbon and glass [1], which could reduce the overall weight and improve the specific stiffness and strength of the composites. For instance, the specific stiffness of flax/polypropylene (PP) was reported to be higher than glass/PP, however, still lower than carbon/PP [1]. Carbon fibre has also been reported to have an outstanding mechanical performance compared to glass fibre [2]. Because of this, hybridisation of flax and carbon fibres becomes one attractive alternative because it reduces the consumption of carbon fibres while achieving reasonably good physical and mechanical properties for the composites.

In addition, composite structures used in outdoor applications are inevitably exposed to environmental attacks, which include temperature and moisture. The environmental attack has been generally known to deteriorate the mechanical properties of the composites. For example, Ridzuan et al. [3] studied the influence of distilled water up to 50 h on the mechanical degradation of hybrid Pennisetum purpureum/glass–epoxy composites. The hybrid composites were prepared at 70 vol% of epoxy and 30 vol% of fibre. Five

✉ K. J. Wong
wongkingjye@curtin.edu.my

1 Quality Engineering Research Cluster (QEREC), Quality Engineering Section, Malaysian Institute of Industrial Technology, Universiti Kuala Lumpur, 81750 Masai, Malaysia

2 Faculty of Mechanical Engineering, Universiti Teknologi Malaysia, 81310 Johor Bahru, Malaysia

3 Automotive Development Centre, Institute for Vehicle Systems and Engineering (IVeSE), Universiti Teknologi Malaysia, 81310 Johor Bahru, Malaysia

4 Department of Mechanical Engineering, Faculty of Engineering and Science, Curtin University Malaysia, 98009 Miri, Malaysia

proportions of the Pennisetum purpureum/glass fibres were prepared, which were 30/0, 24/6, 18/12, 12/18, and 6/24. For both tensile and flexural tests, the strength and modulus were significantly degraded except for flexural modulus on 24/6 and 18/12. The largest percentage degradation was attained in the composite with the highest Pennisetum purpureum.

In contrast, the lowest degradation was found in the composite with the highest glass fibre volume, except for flexural modulus. Karimzadeh et al. [4] studied the tensile and flexural properties of pineapple leaf (PALF) and glass fibre-reinforced epoxy composites that were immersed continuously in distilled water at 60 °C. Four different types of four-ply composites were prepared: pure PALF composite (4P) and three hybrid PALF/glass fibre composites (PGGP, GPPG, and PGPG), with P and G referred to as PALF and glass fibre, respectively. Results showed that the maximum moisture content in 4P was 18.55%, while it was similar in all three types of hybrid composites, ranging from 10.31 to 11.95%. In addition, it was apparent that the tensile strength, tensile modulus, flexural strength, and flexural modulus deteriorated upon moisture attack.

Nevertheless, it was not necessary that 4P experienced the largest percentage of degradation. Maslinda et al. [5] investigated the tensile and flexural properties of woven kenaf/kenaf (KK), jute/jute (JJ), hemp/hemp (HH), interwoven kenaf/jute, and interwoven kenaf/hemp (KH) composites subjected to tap water immersion at room temperature. The strength and modulus dropped for both tensile and flexural tests, while the failure strain was enhanced. The findings above suggested that natural fibres were generally sensitive to moisture attack. Hence, it is essential to investigate the mechanical performance of natural fibre-reinforced composites under moisture attack. Normally, the residual properties are related to the amount of moisture content absorbed into the materials [5, 6]. Hence, the moisture absorption behaviour must be characterised before the mechanical testings.

Fick's law of diffusion is the most common model to chractise the moisture absorption behaviour. Nevertheless, non-Fickian behaviour was also commonly observed in polymer composites. Various models have been proposed to characterise non-Fickian behaviour. Among them, the thickness-dependent model has shown its capability to characterise epoxy moulding compounds (EMCs) [7], woven glass and woven carbon-reinforced epoxy composites [8] and unidirectional carbon/epoxy composites [9]. Based on the previous findings, it was found that by normalising the non-Fickian parameters, a single set of data could fit all the data for the various epoxy-based materials at different thicknesses. It is a great advantage, as it significantly reduces the need for extensive moisture absorption tests. Nevertheless, this model has not yet been implemented in hybrid composites.

In this study, the moisture absorption behaviour of woven carbon, woven flax, and hybrid carbon/flax-reinforced epoxy composites was first characterised. Three-ply composites with four types of stacking sequences were fabricated: CCC, CFC, FCF, and FFF, with C indicating carbon and F indicating flax. All composites were continuously immersed in distilled water at 60 °C. The moisture uptake characteristics were fitted using either Fickian or non-Fickian model, depending on the suitability based on the experimental observation. The moisture absorption parameters were also calculated. In addition, tensile tests were carried out on dry and wet specimens (100 h of immersion). The specific tensile strength, stiffness, and failure were then compared. Finally, the modified Halpin–Tsai equation estimated the stress transfer efficiency parameter, while the modified Chokshi–Chaudhary–Gohil equation predicted the interphase volume fraction for the hybrid composites.

2 Materials and Methods

2.1 Preparation of Composite Specimens

The reinforcements used in this study were 200 g/m^2 plain weave 2/2 carbon fabric and 200 g/m^2 twill weave 2/2 flax fabric. As for the resin, 1006 epoxy resin was used. Both types of fabrics were cut into 250 × 250 mm^2 sizes to fabricate the composite plates. Secondly, the epoxy resin was mixed with hardener at a ratio of 10:6 and stirred gently. Next, the mixture was rolled on the fabrics layer by layer. The laminates were cured using the vacuum bagging method at room temperature for 24 h. Composite plates with four different stacking sequences were prepared: CCC, CFC, FCF, and FFF, where C refers to carbon and F indicates flax. The stacking sequences consider both possibilities of the symmetric stacking sequences of the hybrid composites. The thickness for each composite type, h is reported in Table 1.

The same approach as reported in [10] was adopted to estimate the fibre volume fraction. First, the weights of the epoxy resin and hardener (mixed at a ratio of 10:6), glass fabrics, and flax fabrics were measured. After that, the volume of each constituent was calculated by dividing the

Table 1 Thickness and fibre volume fraction for the plain-woven glass/epoxy and carbon/epoxy composites

Stacking sequence	h (mm)	V_f	ρ (g/cm^3)
CCC	0.66	0.3196	1.31
CFC	0.99	0.3317	1.28
FCF	1.49	0.3438	1.25
FFF	1.50	0.3559	1.23

weight by the density of each constituent. The total volume of the composite was obtained by summing up the volume of each constituent. Subsequently, the fibre volume fraction, V_f was estimated by dividing the fibre volume by the composite volume, as in Table 1. The determination of V_f is essential because the mechanical properties of the composites are directly influenced by the fibre volume fraction [11].

The density, ρ of each type of composites was estimated using the following equation:

$$\rho_c = \rho_m V_m + \rho_{cf} V_{cf} + \rho_{ff} V_{ff} \quad (1)$$

the subscripts *c*, *m*, *cf,* and *ff* refer to composite, matrix, carbon fibre, and flax fibre, respectively. Based on the datasheet provided by the suppliers, the density of the resin and hardener was 1.1 g/cm^3 and 1.03 g/cm^3, respectively. The estimated matrix density is thus 1.07 g/cm^3. In addition, the density of the carbon and flax fabrics, according to the suppliers, is 1.8 g/cm^3 and 1.5 g/cm^3, respectively. It is worth to note that the value of 1.5 g/cm^3 is the common reported density for flax fibre as summarised by Chokshi et al. [12]. The estimated density for each type of composite is listed in Table 1. The density of the composite is decreasing when the flax content increases.

2.2 Moisture Absorption Test

Upon completing the curing process, the composites were cut into specimens of 50 × 50 mm^2 size. Five traveler coupons were prepared for each thickness. The edges of all coupons were not sealed because the side length to thickness ratio is more than 100:1, where the water ingression through edges is negligible, as recommended by ASTM D5229 [13]. In this regard, the water ingression could still be assumed to be one-dimensional through the surface. Then, the specimens were heated in an oven at 60 °C for approximately 18 h, ensuring the fabrication-induced moisture was completely removed from the coupons. All specimens were weighed and recorded as baseline mass after that. To accelerate the ageing process, the coupons were then immersed in an environmental chamber filled with distilled water at 60 °C.

At each time interval, coupons were taken from the water bath and placed in a sealed plastic bag. After that, one specimen was taken out from the plastic bag and wiped using a towel until the surface was free of moisture. The specimen was weighed immediately for three measurements using a three-decimal place digital balance to record the current weight of the coupons. Subsequently, the specimen was placed back into the plastic bag. Similar steps were performed until all specimens were weighed. Then, all specimens were placed back into the water bath. For each specimen, measurements were done within 5 min. As for the entire weighing process of all specimens, it was less than 25 min. This was to avoid significant loss of weight gain when the specimens were outside the water bath. The distilled water was refilled once per week to ensure that the water level was always sufficient to cover all specimens.

2.3 Tensile Test

The composites were cut into specimens at 250 × 25 mm^2. Tensile test was conducted using Instron Universal Testing Machine 5982. All tests were conducted at 1 mm/min under ambient conditions. It is noted that natural fibres could be sensitive to strain rate [14]. Nevertheless, despite ASTM D3039 [15] recommends the testing speed at 2 mm/min, Berges et al. [16] reported that the speeds of 2 mm/min and 1 mm/min have insignificant influence on the tensile properties of flax/epoxy composites. An extensometer of 50 mm gauge length was attached to the middle section of the specimen to measure local displacement during testing. Five replicates were tested for each set of specimens. Altogether there were eight sets of specimens, which were CCC, CFC, FCF, and FFF, under both dry and wet conditions. For wet specimens, tensile tests were conducted immediately after the specimens were taken out from the water bath after 100 h of immersion.

3 Results and Discussion

3.1 Moisture Absorption Curves

Figure 1 plots the average moisture absorption curves of the composites with four different stacking sequences. The error bars indicate the standard deviation based on the moisture absorption data measured at each interval. It is noticed that for all composites, the moisture absorption increases linearly at the initial stage and gradually slows down afterward.

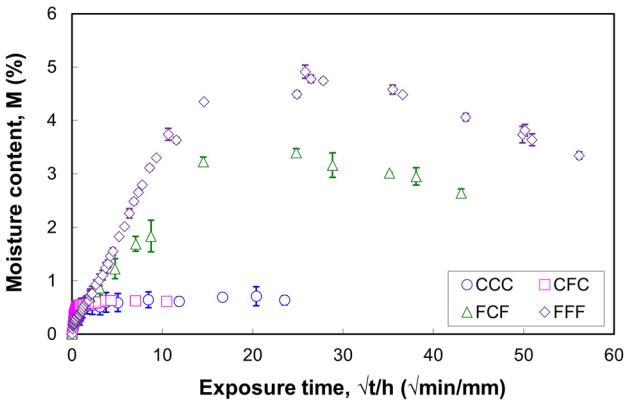

Fig. 1 Moisture absorption curves of CCC, CFC, FCF, and FFF composites

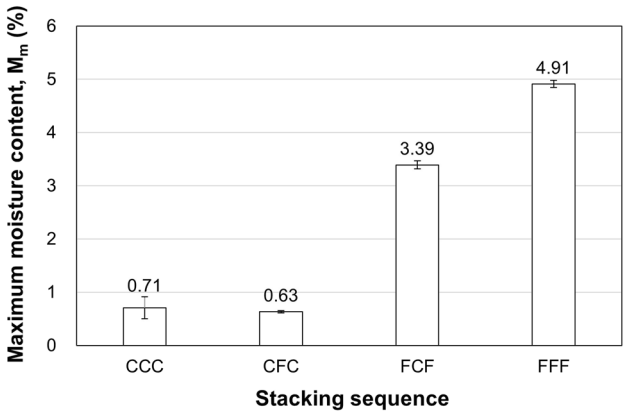

Fig. 2 Maximum moisture absorption content of CCC, CFC, FCF, and FFF composites

Subsequently, the saturation is reached, and the moisture absorption curve levels off. For FCF and FFF, there is a decrement in the moisture content beyond the maximum moisture content. This is most likely to be attributed to the combined effect of the local fracture of the matrix due to different rates of swelling, which is caused by the difference in the hygrothermal properties between the constituents [17], removal of uncrosslinked epoxy molecules [18], and the leaching of the water-soluble substance from the flax fibre [19]. Dissolution of pectins from the flax fibre surface upon distilled water immersion has also been observed by Bourmaud et al. [20] and Le Duigo et al. [21]. Consequently, voids might be developed at the fibre/matrix interface, leading to micro-cracks formation and accumulation.

In addition, the maximum moisture content for different types of composites varies from each other. Figure 2 displays the average maximum moisture content M_m of all four types of composites. Considering the standard deviation of the data as indicated by the error bars, the M_m for CCC and CFC can be viewed as the same. This observation suggests that the carbon fabrics at the outer layer have restricted further moisture absorption into the middle flax fabric layer. A significant difference is observed for FCF and FFF, where the average M_m is 3.39% and 4.91%, respectively. Compared to CCC, there is an approximately 5 and 7 times increment in the maximum moisture content in FCF and FFF, respectively. The observation suggests that the moisture absorption content in flax fabric is higher than in carbon fabric, which is attributed to the hydrophilic nature of the natural fibre. It is also generally supported by other researchers [3, 4]. It is also worth noting that as flax fabric is sensitive to moisture absorption, the inner layer of FFF still plays a significant role in absorbing the water molecules.

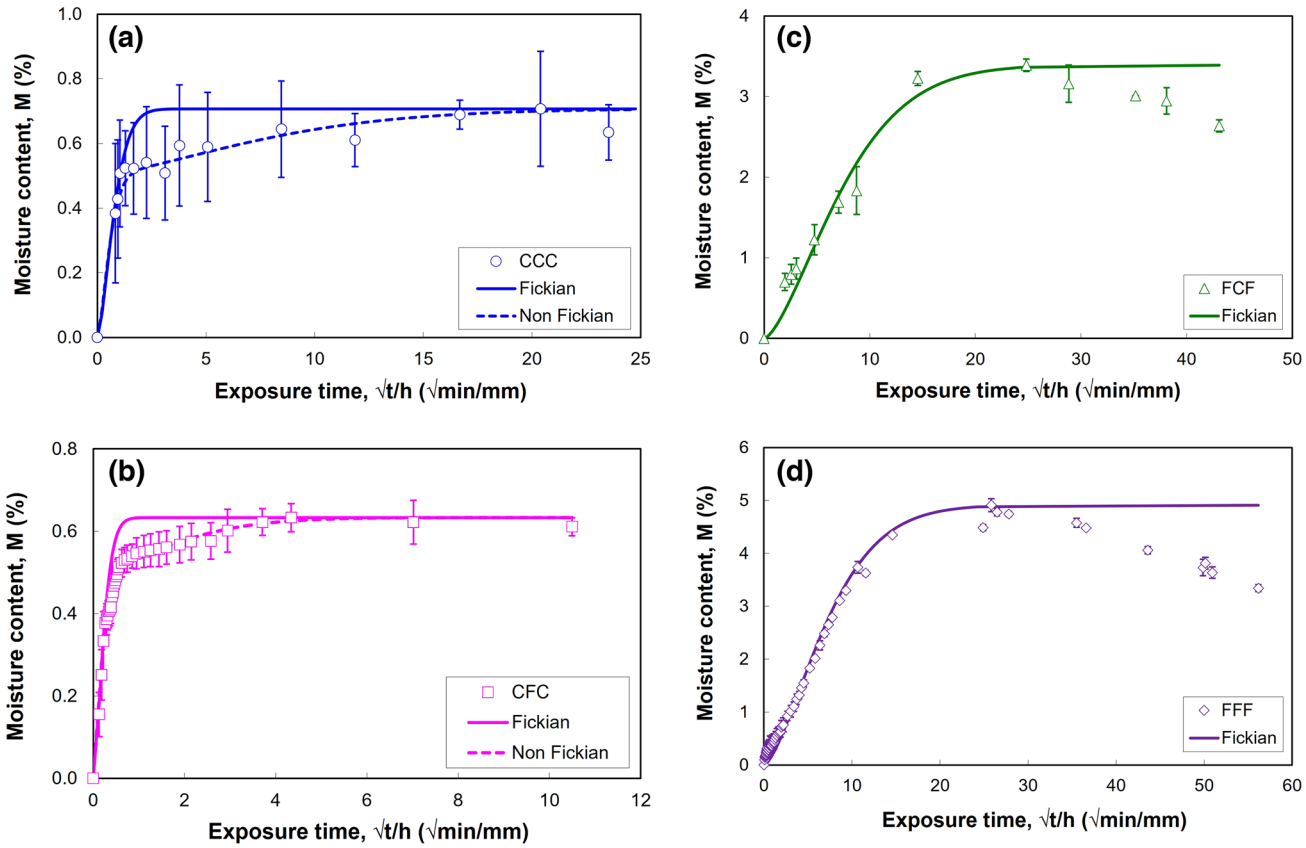

Fig. 3 Experimental and fitted moisture absorption curves for **a** CCC, **b** CFC, **c** FCF and **d** FFF composites

3.2 Fickian Diffusion Model

To characterise the moisture absorption behaviour as a function of time, the moisture absorption data in Fig. 1 is further analysed using the Fickian moisture diffusion model, which reads:

$$M(t) = M_m\left\{1 - exp\left[-7.3\left(\frac{D_z t}{h^2}\right)^{0.75}\right]\right\} \tag{2}$$

In Eq. (2), $M(t)$ is the moisture content at any instant, M_m refers to maximum moisture content, t indicates the exposure time at any instant, and h is the thickness of the specimens. D_z implies the diffusivity, which is described by:

$$D_z = \pi\left(\frac{h}{4M_m}\right)^2\left(\frac{M_2 - M_1}{\sqrt{t_2} - \sqrt{t_1}}\right)^2 \tag{3}$$

The expression $(M_2 - M_1)/(\sqrt{t_2} - \sqrt{t_1})$ refers to the slope of the initial linear region of the moisture absorption plot. The characterisation of D_z provides an important information on the rate of moisture uptake in the material. A larger value of diffusivity implies that the material is more susceptible to moisture absorption and vice-versa. The solid lines in Fig. 3 show the moisture absorption curves generated using the Fickian diffusion model. It is to note that the y-axis of the four types of composites shown in Fig. 3 is not plotted at the same scale for better visualisation of the experimental and fitted plots. It is noticed that Fickian diffusion fails to describe the moisture absorption behaviour in CCC and CFC composites. Nevertheless, it fits well with the FCF and FFF composites. It has also been reported that the water uptake of unidirectional flax/epoxy composites subjected to 70 °C/85%RH was well fitted using Fick's law [16]. It is to note that the Fickian diffusion model does not consider the decrement in the moisture level beyond the maximum moisture content. The D_z values for FCF and FFF are similar, which are 0.95×10^{-3} and 1.03×10^{-3} mm^2/min, respectively. This suggests that the outer flax layers dominate the diffusivity. The D_z values for CCC and CFC are not reported because they exhibit non-Fickian behaviour, which requires a different model for fitting, and will be discussed in the following section.

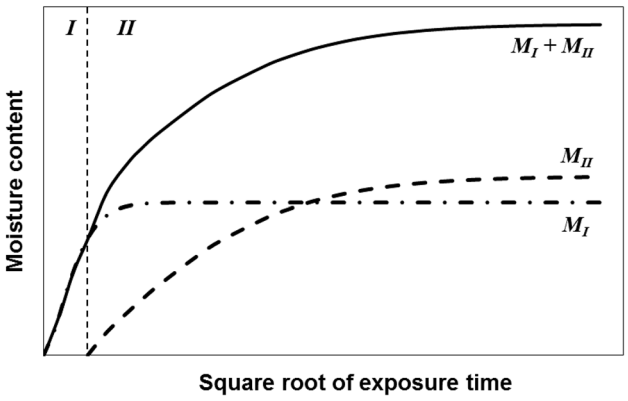

Fig. 4 Moisture absorption distribution of Stage I (M_I), Stage II (M_{II}), and superimposed diffusion ($M_I + M_{II}$) of the non-Fickian model

3.3 Non-Fickian Model

A non-Fickian model is required when the moisture absorption does not follow Fickian behaviour. The non-Fickian models are usually developed by modifying the Fickian diffusion model. Some common non-Fickian models include Sequential Dual Fickian (SDF) [22], Delayed Dual Fickian (DDF) [23], Parallel Dual Fickian (PDF) [24–26] and Langmuir [27–31] models. The two-stage non-Fickian model used in this study is described in Fig. 4. This model has been successfully implemented in epoxy moulding compounds (EMCs) [7], woven glass and carbon-reinforced epoxy composites [8] and unidirectional carbon/epoxy composites [9]. Stage I indicates Fickian diffusion, while Stage II describes non-Fickian behaviour. The total moisture is obtained by superimposing the moisture content at both stages.

Mathematically, the non-Fickian model is described as follows:

$$\begin{aligned} M(t) &= M_I(t) + M_{II}(t) \\ &= M_{m,F}G(t) + \left(M_m - M_{m,F}\right)W(t) \\ &= M_{m,F}\left\{1 - \exp\left[-7.3\left(\frac{D_z t}{h^2}\right)^{0.75}\right]\right\} \\ &+ \left(M_m - M_{m,F}\right)\left\{1 - \exp\left[-\left(\alpha\langle t - t_o\rangle\right)^{0.75}\right]\right\} \end{aligned} \tag{4}$$

In Eq. (4), $M_{m,F}$ and M_m refer to Stage I and superimposed maximum moisture content, respectively, D_z refers to the diffusivity during the Fickian stage, h is the thickness of the specimens, and t implies the instantaneous aging period. In addition, t_o signifies the initiation time of the non-Fickian behaviour, and α indicates the non-Fickian diffusivity per square thickness. The Macaulay bracket $\langle\cdot\rangle$ for the time delay term $\langle t - t_o\rangle$ implies that non-Fickian behaviour starts when $t \geq t_o$. This model has been successfully implemented to characterise the non-Fickian moisture absorption behaviour in various materials [7–9].

The steps to implement the non-Fickian model are described as follows:

(i) Estimate $M_{m,F}$ as the value at the deviation from the linear line.

(ii) Calculate D_z by using Eq. (3). It is to note that since it refers to the diffusivity at Stage I, hence $M_{m,F}$ should be used instead of M_m.
(iii) Generate the Stage I moisture absorption data $M_I(t)$ using the first part of Eq. (4).
(iv) Subtract the experimental moisture content $M(t)$ from the $M_I(t)$ to obtain the experimental $M_{II}(t)$.
(v) Determine the experimental $W(t)$ using Eq. (5) below:

$$W(t) = \frac{M(t) - M_I(t)}{M_m - M_{m,F}} \tag{5}$$

(vi) Identify t_o, which is the corresponding immersion time when $M_{m,F}$ is attained.
(vii) Plot the curve of $W(t)$ versus $t - t_o$, and obtain the best-fit α using the expression $1 - \exp\left[-\left(\alpha\langle t - t_o\rangle\right)^{0.75}\right]$.

Table 2 lists the non-Fickian parameters for both CCC and CFC. It is worth noting that the $M_{m,F}$ for both stacking sequences are estimated to be the same. Nevertheless, the values of D_z and α of CFC are an order higher than CCC. This indicates that in both Fickian and non-Fickian regions, the diffusion rate in CFC is slower than in CCC. In addition, CFC ($t_o = 17$ s) enters non-Fickian region faster than CCC ($t_o = 28$ s). It is reasonable due to the larger D_z in CFC. While the diffusion rate is faster, CFC would enter the non-Fickian region at a shorter period. Higher moisture content would lead to more severe degradation in the mechanical properties of the materials. The dashed lines plot the fitted curves in Fig. 3a and b. Results show good fits of the experimental data using the non-Fickian model.

3.4 Tensile Properties

Figure 5 displays the tensile stress–strain curves of CCC, CFC, FCF, and FFF composites under dry and wet conditions. In both dry and wet conditions, the CCC, CFC, and FCF composites exhibit linear elastic behaviour up to the tensile strength. This indicates the brittle behaviour of the three types of composites. Nevertheless, for FFF, significant nonlinearity is observed. An enlarged view of FFF is also shown in Fig. 5 for better visualisation of the nonlinearity of both dry and wet specimens.

Table 2 Non-Fickian parameters for the CCC and CFC composites

Stacking sequence	$M_{m,F}$ (%)	D_z (mm^2/min)	t_o (s)	α ($\times 10^{-1}$ min^{-1})
CCC	0.5	0.17	28	0.277
CFC	0.5	1.53	17	2.089

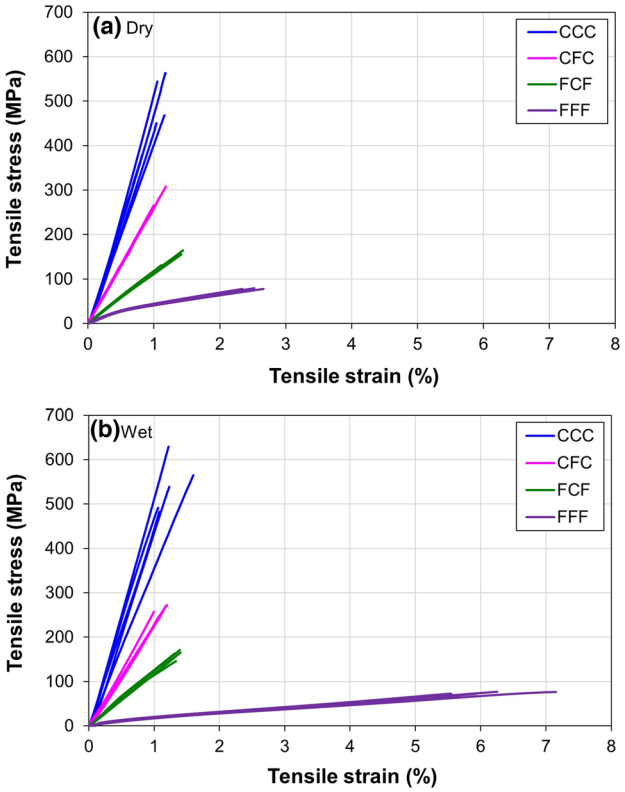

Fig. 5 Tensile stress–strain behaviour of CCC, CFC, FCF, and FFF composites at **a** dry and **b** wet conditions

The first approximate linear region within the range of 5–20 MPa is taken for dry and wet specimens to calculate the tensile modulus for FFF. The specific tensile moduli for all four types of composites are plotted in Fig. 6. The specific property (property per unit density) is presented for a meaningful direct comparison among the four composites. The error bars indicate the standard deviation for each set of data. The average value is also indicated for ease of

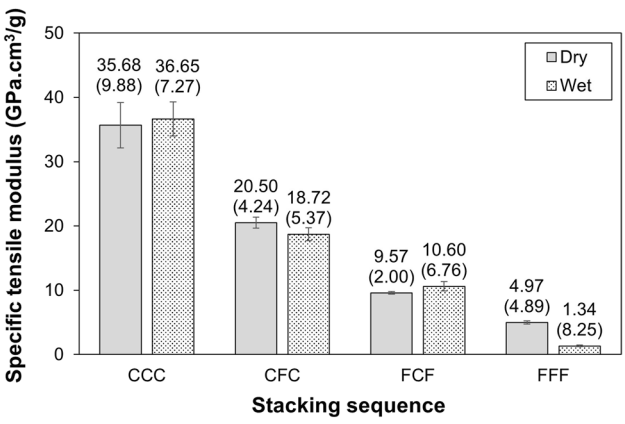

Fig. 6 Specific tensile modulus of dry and wet specimens for CCC, CFC, FCF, and FFF composites

reference. In addition, the values in the bracket are the coefficient of variation in %. Results show good repeatability with a maximum coefficient of variation of less than 10%. For dry and wet specimens, it is apparent that CCC has the highest tensile modulus, followed by CFC, FCF, and FFF. The trend shows the positive effect of the hybridisation of flax and carbon fibres, where the hybrid composites exhibit an enhanced stiffness compared to neat flax fibre composites. In addition, considering the standard deviation range shown as the error bars, the tensile modulus for dry and wet CCC is constant. This is because carbon fibre is commonly considered inert to moisture attack [6].

On the other hand, FFF has attained the largest drop of 73% in the specific tensile modulus upon moisture absorption. Because flax fibre is hydrophilic [32], moisture absorption causes significant plasticisation in the fibre. The reduction in the tensile modulus upon water absorption could be attributed to the formation of the hydrogen bonds (due to high polar components of the surface energy in flax fibres) that deteriorated the interfacial adhesion at the fibre/matrix interface [5, 33]. Water molecules might also weaken the interactions between crystalline and amorphous zones in the flax fibres, which deteriorates the interfacial bonding and decreases the tensile modulus [21, 34, 35].

In addition, a slight decrement of 9% in the specific tensile modulus for CFC and a slight increment of 11% in the specific tensile modulus of wet FCF. A slight increment in the specific tensile modulus could be caused by the relaxation of the thermal residual stress upon water absorption. The retention in the tensile modulus in the hybrid composites highlights the positive effect of the hybridisation of natural fibre with synthetic fibre. Ridzuan et al. [3] have also observed the degradation in the mechanical properties due to water absorption became less severe when *Pennisetum Purpureum* grass fibre was hybridised with glass fibre. Not only that, it is believed that symmetric laminates help retain the tensile properties upon moisture attack. It is because, in an unbalance laminate, the difference in the hygrothermal properties of the fibres would cause natural curvature in the composite. Consequently, during the mounting of the specimens for the tensile test, there is already pre-stressed induced in the specimens. This has also been observed by Karimzadeh et al. [4], whereupon distilled water absorption of hybrid pineapple leaf (P) and glass (G) fibre composites, the symmetric stacking sequences (PGGP and GPPG) would retain the tensile modulus and strength better than the alternating stacking sequence (PGPG).

Figure 7 compares the specific tensile strength of the four types of composites. Generally, good repeatability is obtained, where the coefficient of variation is less than 10%, except for CCC dry and wet composites. Similar to the tensile modulus, the positive influence of carbon fibres in enhancing the tensile strength of the flax fibre

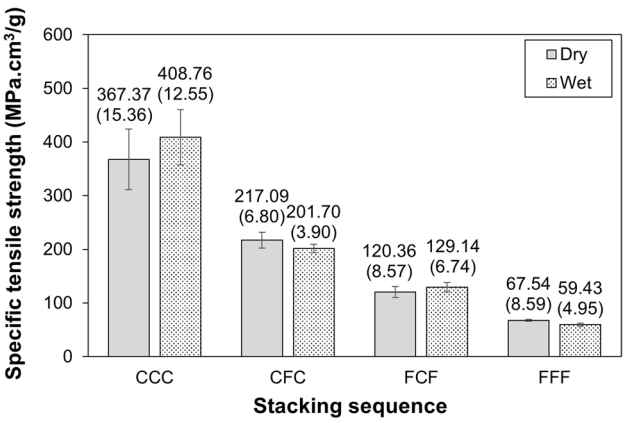

Fig. 7 Specific tensile strength of dry and wet specimens for CCC, CFC, FCF, and FFF composites

composite is also noticed in both hybrid composites. Considering the standard deviation of both CCC composites, the tensile strength could be invariant because the error bars have covered the range of the average values of both composites. For CFC, there is an average 7% drop in the specific tensile strength. As for FCF, it has also attained a slight increment in the specific tensile strength. The observation of the specific tensile strength for CCC, CFC, and FCF is similar to the specific tensile modulus, which is believed to be attributed to the same reasons described in the previous paragraphs. The tensile strength of the composites could be further enhanced by incorporating fly-ash [36] or Roselle (*Hibiscus sabdariffa*) waste powder [37] into the composites.

Nevertheless, unlike specific tensile modulus, the specific tensile strength of FFF is relatively stable upon moisture attack, where there is only a 12% decrement in the wet specimens. This could be even though water molecules have weakened the interfacial bonding behaviour of the flax fibre with the matrix. They do not significantly deteriorate the tensile strength of the flax fibres. In some cases, it was found that the tensile strength of the unidirectional flax/epoxy composites has attained a slight increment after moisture absorption [16, 38].

As for the specific tensile failure strain, Fig. 8 shows that it is practically invariant in CCC, CFC, and FCF composites for both dry and wet specimens. This indicates that the tensile failure strain of the carbon fibre is the limiting value for the composites that contain carbon fabric. This is reasonable because, during tensile loading, the iso-strain condition will cause all constituents to displace at the same rate. While the carbon fibre has a smaller tensile failure strain than the flax fibre (Fig. 8), the carbon fibre will control the overall tensile strain of the composite. Nevertheless, it is worth noting that when the number of flax fabrics is larger (FCF), the tensile failure strain is slightly increased. This is reasonable because

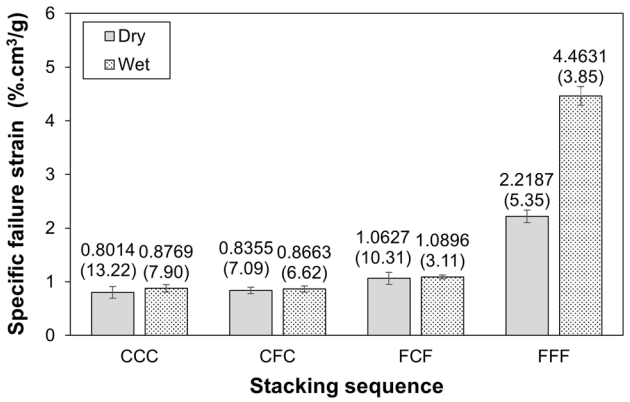

Fig. 8 Specific tensile failure strain of dry and wet specimens for CCC, CFC, FCF, and FFF composites

the only inner carbon fabric in FCF cannot dominate the tensile strain as much as in the cases in CCC and CFC. On the other hand, the failure strain is found to be doubled in FFF. The possible reasons are related to the observation in the tensile modulus, where the plasticisation of the flax fibre and dissolution of the pectins from the flax fibre would have enhanced the flexibility of the fibre [4, 5, 16].

3.5 Modified Halpin–Tsai Equation

The tensile modulus and strength of fitted using the modified Halpin–Tsai equation for hybrid composites [39]. The following procedures were employed to estimate the tensile properties of the hybrid composites.

(i) Estimate the tensile modulus and strength of the carbon and flax fibres using the properties of non-hybrid composites (CCC and FFF):

$$E_c = E_m(1 - V_f) + E_f V_f \tag{6}$$

$$S_c = S_m(1 - V_f) + S_f V_f \tag{7}$$

Table 3 Tensile modulus and strength for the epoxy, CCC, and FFF at dry and wet conditions. [40]

Material	Dry		Wet	
	E (GPa)	*S* (MPa)	*E* (GPa)	*S* (MPa)
Epoxy	1.58[a]	30[a]	0.63[b]	12[b]
CCC	46.74	481.26	48.01	535.47
FFF	6.12	83.08	1.64	73.10

[a]From manufacturer.

[b]Estimated by assuming 20% of the properties is retained upon water immersion [43]

Table 4 Tensile modulus and strength for the carbon and flax fibres in dry and wet conditions

Fibre	Dry		Wet	
	E (GPa)	*S* (MPa)	*E* (GPa)	*S* (MPa)
Carbon	142.90	1442.06	148.89	1650.03
Flax	14.33	179.14	3.48	183.66

where E refers to the tensile modulus, S is the tensile strength, V is the volume fraction. The subscripts c, m, and f refer to the composite (CCC or FFF), matrix (epoxy), and fibre (carbon or flax), respectively. Using the fibre volume fraction in Table 1 and the data listed in Table 3, the properties of the fibres are estimated (Table 4).

(ii) Estimate the curve-fitting parameter ξ of the modified Halpin–Tsai equation:

$$E_c = E_m\left[\frac{1 + \xi(\eta_{cf}V_{cf} + \eta_{ff}V_{ff})}{1 - (\eta_{cf}V_{cf} + \eta_{ff}V_{ff})}\right] \tag{8}$$

where

$$\eta_{cf} = \frac{\left(\frac{E_{cf}}{E_m}\right) - 1}{\left(\frac{E_{cf}}{E_m}\right) + \xi} \tag{9}$$

$$\eta_{ff} = \frac{\left(\frac{E_{ff}}{E_m}\right) - 1}{\left(\frac{E_{ff}}{E_m}\right) + \xi} \tag{10}$$

In the above equations, the subscripts *cf* and *ff* refer to the carbon and flax fibres, respectively, while η indicates the stress transfer efficiency parameter, which ranges between zero and unity. Although this model was originally developed to evaluate the transverse properties, it has also been attempted for woven fabric composites [41]. It is also worth noting that in the original formulation of the Halpin–Tsai equation, ξ is called the shape fitting parameter, which describes the packing arrangement and the geometry of the fibre [42]. In view of this, this parameter does not seem to have a direct physical meaning for woven composites used in this study and hence is treated as a fitting parameter that contributes to the efficiency parameter η. In addition, Eq. (8) can also be implemented to estimate the tensile strength [41] by replacing the modulus E with the strength S values.

Using the fibre volume fraction listed in Table 1 and the mechanical properties of the hybrid composites, which are determined experimentally (Table 5), the fibre volume fraction for each type of fibre as well as the best-fit parameters ξ and η are as indicated in Table 6 and Table 7 below.

From the values shown in Tables 6 and 7, it can be noticed that η_{ff} is significantly smaller than η_{cf} for both CFC and FCF under dry and wet conditions. The trend indicates that the tensile modulus and tensile strength of the hybrid composites are mainly controlled by carbon fibre, which could be attributed to flax's significantly low tensile properties compared to carbon fibre (Table 4). For CFC, η_{cf} is considerably stable after water immersion. However, it decreases in FCF. This is probably because there are more flax layers than carbon in FCF. While flax fibre is sensitive to water attack, water immersion significantly affects the flax/carbon interface quality, thus reducing the efficiency parameter. It is also worth noting that the reduction in η_{cf} is 51.15% for tensile modulus and 26.81% for tensile strength. This is reasonable as water immersion significantly influences the tensile modulus in flax fibre compared to the tensile strength (Tables 3 and 4). Treatment of the flax fibre, such as alkali treatment, could be one possibility to enhance the stress transfer efficiency to achieve an overall improvement in the mechanical properties of the composites [43–47].

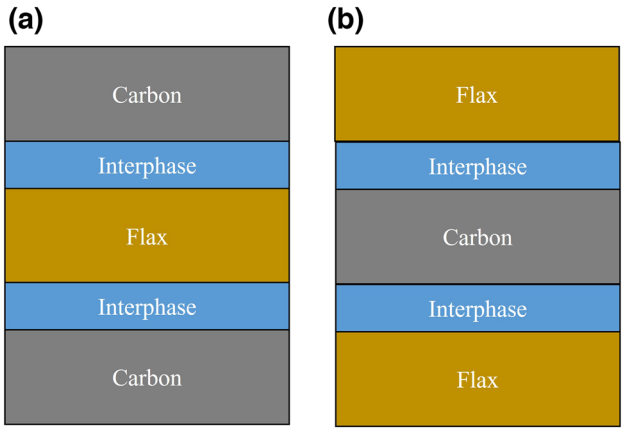

Fig. 9 Schematic diagram of the interphase between carbon and flax fibres for **a** CFC and **b** FCF hybrid composites

3.6 Modified Chokshi–Chaudhary–Gohil Equation

The tensile modulus of both CFC and FCF hybrid composites is also further analysed using the modified Chokshi–Chaudhary–Gohil Equation [48]. It is noted that the original equation was developed to analyse the interphase between the fibre and matrix. In this study, the equation is modified to analyse the interphase between the two types of fibres (Fig. 9). Hence, some assumptions and modifications

Table 5 Tensile modulus and strength of CFC and FCF in dry and wet conditions

Composite	Dry		Wet	
	E (GPa)	*S* (MPa)	*E* (GPa)	*S* (MPa)
CFC	26.24	277.88	23.96	258.18
FCF	11.97	150.45	13.25	161.42

Table 6 The best-fit parameters for the tensile modulus of the hybrid composites at dry and wet conditions

Composite	Fibre volume fraction*		Dry			Wet		
	V_{cf}	V_{ff}	ξ	η_{cf}	η_{ff}	ξ	η_{cf}	η_{ff}
CFC	0.2131	0.1186	227	0.2819	0.0342	489	0.3239	0.0091
FCF	0.1065	0.2373	73	0.5474	0.0984	642	0.2674	0.0070

*The fibre volume fraction for one layer of each type of fibre is estimated by dividing the V_f of CCC or FFF (Table 1) by the total number of layers (i.e. 3)

Table 7 The best-fit parameters for the tensile strength of the hybrid composites in dry and wet conditions

Composite	Fibre volume fraction*		Dry			Wet		
	V_{cf}	V_{ff}	ξ	η_{cf}	η_{ff}	ξ	η_{cf}	η_{ff}
CFC	0.2131	0.1186	41	0.6806	0.1612	120	0.6599	0.0359
FCF	0.1065	0.2373	23	0.7886	0.2517	171	0.5771	0.0255

Table 8 The best-fit parameters for the interphase volume fraction and the percentage error for the predicted composite tensile modulus of the hybrid composites in dry and wet conditions

Composite	Volume fraction			Dry			Wet		
	V_i	V_{cf1}	V_{ff1}	Exp	Ana	% diff	Exp	Ana	% diff
CFC	0.08	0.1597	0.0920	26.24	25.32	3.50	23.96	24.57	2.56
FCF	0.11	0.0699	0.1639	11.97	13.54	13.15	13.25	11.46	13.56

have been made to implement the Chokshi–Chaudhary–Gohil Equation:

(i) The dominant interphase is assumed to be formed between the two types of fibres due to the incompatibility between the synthetic and natural fibres.

(ii) The interphase stiffness E_i is assumed to be the stiffness of the matrix E_m based on the assumption that both layers of fibres are joined by the epoxy resin. In accordance with Table 3, $E_i = 1.58$ GPa and 0.63 GPa for dry and wet resin, respectively.

(iii) The stiffness of the hybrid composite is estimated using:

$$E_c = E_m(1 - V_f) + E_{cf}V_{cf1} + E_{ff}V_{ff1} + E_iV_i \quad (11)$$

where the subscript 1 refers to the new fibre volume fraction after deducting the interface volume fraction according to the ratio of the number of layers for each type of fibre:

$$V_{cf1} = V_{cf} - \frac{n}{3}V_i \quad (12)$$

$$V_{ff1} = V_{ff} - \frac{n}{3}V_i \quad (13)$$

V_{cf} and V_{ff} for both CFC and FCF are shown in Tables 6 and 7. The term n refers to the number of layers for each type of fibre. For CFC, $n = 2$ for carbon and $n = 1$ for flax, while $n = 1$ for carbon and $n = 2$ for flax for FCF. This assumes that each layer for both types of fibres contributes equally to the total thickness of the interphase Table 8.

(iv) Substituting Eqs. (12) and (13) into Eq. (11), there is only one unknown left, which is V_i. Table 8 lists the best-fit V_i and the corresponding V_{cf1} and V_{ff1} for both CFC and FCF. The maximum percentage error of the composite tensile modulus E_c is less than 14%, which reflects a comparatively good fit. Based on the results, the interphase volume fraction V_i is estimated to be 8% and 11% for CFC and FCF, respectively. When V_i is related to V_f using the following equation [49], the value of x is estimated to be 0.24 and 0.32 for CFC and FCF, respectively. These values suggest that the carbon/flax interphase to total fibre ratio is 24% and 32% for CFC and FCF, respectively.

$$V_i = xV_f \quad (14)$$

4 Conclusions

This study conducted the moisture absorption characteristics and tensile behaviour of carbon (C), flax (F), and hybrid carbon/flax reinforced epoxy composites. Three-ply composites with four different stacking sequences were studied: CCC, CFC, FCF, and FFF. Based on the results, the following could be concluded:

(i) As the outer layer, carbon could significantly reduce the maximum moisture content.

(ii) The moisture absorption in FCF and FFF followed Fick's law with a similar diffusivity value. On the other hand, CCC and CFC were well-fitted using a non-Fickian model, where the diffusivity in CFC appeared to be an order higher than CCC.

(iii) From tensile tests, it is apparent that carbon fibre exhibited higher specific strength and modulus but lower failure strain than flax fibre.

(iv) Upon moisture attack, the tensile strength was retained for all four stacking sequences. As for the tensile modulus and failure strain, an insignificant influence was observed in CCC, CFC, and FCF composites. A significant reduction of 73% in specific tensile modulus and an increment of 101% in specific failure strain was found in FFF.

(v) Fitting the results using a modified Halpin–Tsai equation shows that the carbon fibre mainly contributes to the stress transfer efficiency.

(vi) Based on the modified Chokshi–Chaudhary–Gohil Equation, the best-fit interphase volume fraction was 8% and 11% for CFC and FCF, respectively.

Acknowledgements This work was supported by Universiti Teknologi Malaysia through UTM Fundamental Research (UTMFR) Grant No. Q.J130000.3851.22H02 and No. Q.J130000.3851.21H92.

Data availability The datasets used and/or analysed during the current study are available from the corresponding author on reasonable request.

Declarations

Conflict of Interest The authors declare that there is no actual or potential conflict of interest in relation to this article.

References

1. L. Pil, F. Bensadoun, J. Pariset, I. Verpoest, Why are designers fascinated by flax and hemp fibre composites? Compos. Part A-Appl. S. **83**, 193–205 (2016)
2. S.P. Karjala, V.K. Kuttynadar Rajammal, S. Gopi, R. Ravi, D. Chockalingam, M. Chinathambi Muthukaruppan, Influence of IPNS (vinylester/epoxy/polyurethane) on the mechanical properties of glass/carbon fiber reinforced hybrid composites. IIUM Eng. J. **23**(1), 339–348 (2022)
3. M.J.M. Ridzuan, M.S. Abdul Majid, M. Afendi, K. Azduwin, N.A.M. Amin, J.M. Zahri, A.G. Gibson, Moisture absorption and mechanical degradation of hybrid Pennisetum purpureum/glass–epoxy composites. Compos. Struct. **141**, 110–116 (2016)
4. A. Karimzadeh, M.Y. Yahya, M.N. Abdullah, K.J. Wong, Effect of stacking sequence on mechanical properties and moisture absorption characteristic of hybrid PALF/glass fiber composites. Fibers Polym. **21**(7), 1583–1593 (2020)
5. A.B. Maslinda, M.S. Abdul Majid, M.J.M. Ridzuan, M. Afendi, A.G. Gibson, Effect of water absorption on the mechanical properties of hybrid interwoven cellulosic-cellulosic fibre reinforced epoxy composites. Compos. Struct. **167**, 227–237 (2017)
6. S.F. Mad Asasaari, K.J. Wong, M.N. Tamin, M. Johar, Moisture absorption effects on the mechanical properties of carbon/epoxy composites. Int. J. Struct. Integr. **11**(4), 605–614 (2020)
7. K.J. Wong, K.O. Low, H.A. Israr, M.N. Tamin, Thickness-dependent non-Fickian moisture absorption in epoxy molding compounds. Microelectron. Reliab. **65**, 160–166 (2016)
8. M. Johar, H.S. Kang, W.W.F. Chong, K.J. Wong, A further generalized thickness-dependent non-Fickian moisture absorption model using plain woven epoxy composites. Polym. Test. **69**, 522–527 (2018)
9. A. Azizan, M. Johar, S.S. Karam Singh, S. Abdullah, S.S. Koloor, M. Petrů, K.J. Wong, M.N. Tamin, An extended thickness-dependent moisture absorption model for unidirectional carbon/epoxy composites. Polymers **13**(3), 440 (2021)
10. M. Johar, H.A. Israr, K.O. Low, K.J. Wong, Numerical simulation methodology for mode II delamination of quasi-isotropic quasi-homogeneous composite laminates. J. Compos. Mater. **51**(28), 3955–3968 (2017)
11. S. Chokshi, P. Gohil, D. Patel, Experimental investigations of bamboo, cotton and viscose rayon fiber reinforced unidirectional composites. Mater. Today: Proc. **28**, 498–503 (2020)
12. S. Chokshi, V. Parmar, P. Gohil, V. Chaudhary, Chemical composition and mechanical properties of natural fibers. J. Nat. Fibers **19**(10), 3942–3953 (2022)
13. ASTM D5229, *Standard test method for moisture absorption properties and equilibrium conditioning of polymer matrix composite materials* (ASTM International, West Conshohocken, 2010)
14. S. Chokshi, P. Gohil, A. Lalakiya, P. Patel, A. Parmar, Tensile strength prediction of natural fiber and natural fiber yarn: strain rate variation upshot. Mater. Today: Proc. **27**, 1218–1223 (2020)
15. ASTM D3039, *Standard test method for tensile properties of polymer matrix composite materials* (ASTM International, West Conshohocken, 2008)
16. M. Berges, R. Léger, V. Placet, V. Person, S. Corn, X. Gabrion, J. Rousseau, E. Ramasso, P. Ienny, S. Fontaine, Influence of moisture uptake on the static, cyclic and dynamic behaviour of unidirectional flax fibre-reinforced epoxy laminates. Compos. Part A-Appl. S. **88**, 165–177 (2016)
17. D.A. Bond, P.A. Smith, Modeling the transport of low-molecular-weight penetrants within polymer matrix composites. Appl. Mech. Rev. **59**(5), 249–268 (2006)
18. U. Gaur, B. Miller, Effects of environmental exposure on fiber/epoxy interfacial shear strength. Polym. Compos. **11**(4), 217–222 (1990)
19. Z.N. Azwa, B.F. Yousif, A.C. Manalo, W. Karunasena, A review on the degradability of polymeric composites based on natural fibres. Mater. Des. **47**, 424–442 (2013)
20. A. Bourmaud, C. Morvan, C. Baley, Importance of fiber preparation to optimize the surface and mechanical properties of unitary flax fiber. Ind. Crops Prod. **32**(3), 662–667 (2010)
21. A. Le Duigou, P. Davies, C. Baley, Exploring durability of interfaces in flax fibre/epoxy micro-composites. Compos. Part A-Appl. S. **48**, 121–128 (2013)
22. A. Ameli, N.V. Dalta, M. Papini, J.K. Spelt, Hygrothermal properties of highly toughened epoxy adhesives. J. Adhes. **86**, 698–725 (2010)
23. A. Mubashar, I.A. Ashcroft, G.W. Critchlow, A.D. Crocombe, Moisture absorption-desorption effects in adhesive joints. Int. J. Adhes. Adhes. **29**(8), 751–760 (2009)
24. L.-R. Bao, A.F. Yee, Moisture diffusion and hygrothermal aging in bismaleimide matrix carbon fiber composites. Part II: Woven and hybrid composites. Compos. Sci. Technol. **62**(16), 2111–2119 (2002)
25. W.K. Loh, A.D. Crocombe, M.M. Abdel Wahab, I.A. Ashcroft, Modelling anomalous moisture uptake, swelling and thermal characteristics of a rubber toughened epoxy adhesive. Int. J. Adhes. Adhes. **25**(1), 1–12 (2005)
26. M.D. Placette, X. Fan, J.-H. Zhao, D. Edwards, Dual stage modeling of moisture absorption and desorption in epoxy mold compounds. Microelectron. Reliab. **52**(7), 1401–1408 (2012)
27. Y. Li, J. Miranda, H.-J. Sue, Hygrothermal diffusion behavior in bismaleimide resin. Polymer **42**(18), 7791–7799 (2001)
28. G. LaPlante, A.V. Ouriadov, P. Lee-Sullivan, B.J. Balcom, Anomalous moisture diffusion in an epoxy adhesive detected by magnetic resonance imaging. J. Appl. Polym. Sci. **109**, 1350–1359 (2008)
29. M.H. Lee, N.A. Peppas, Water transport in graphite/epoxy composites. J. Appl. Polym. Sci. **47**, 1349–1359 (1993)
30. S. Popineau, C. Rondeau-Mouro, C. Sulpice-Gaillet, M.E.R. Shanahan, Free/bound water absorption in an epoxy adhesive. Polymer **46**(24), 10733–10740 (2005)
31. V. La Saponara, Environmental and chemical degradation of carbon/epoxy and structural adhesive for adhesive for aerospace applications: Fickian and anomalous diffusion Arrhenius kinetics. Compos. Struct. **93**, 2180–2195 (2011)
32. A. Moudood, A. Rahman, A. Öchsner, M. Islam, G. Francucci, Flax fiber and its composites: an overview of water and moisture absorption impact on their performance. J. Reinf. Plast. Compos. **38**(7), 323–339 (2018)
33. C. Baley, F. Busnel, Y. Grohens, O. Sire, Influence of chemical treatments on surface properties and adhesion of flax fibre–polyester resin. Compos. Part A-Appl. S. **37**(10), 1626–1637 (2006)
34. O.M. Astley, A.M. Donald, A small-angle X-ray scattering study of the effect of hydration on the microstructure of flax fibers. Biomacromol **2**(3), 672–680 (2001)
35. A. le Duigou, A. Bourmaud, E. Balnois, P. Davies, C. Baley, Improving the interfacial properties between flax fibres and PLLA by a water fibre treatment and drying cycle. Ind. Crops Prod. **39**, 31–39 (2012)
36. R. Ganesamoorthy, G. Suresh, K.R. Padmavathi, J. Rajaparthiban, R. Vezhavendhan, G. Bharathiraja, Experimental analysis and

mechanical properties of fly-ash loaded E-glass fiber reinforced IPN (vinylester/polyurethane) composite. Fibers Polym. **23**(10), 2916–2926 (2022)
37. B.V. Dharmendra, S. Vivek, P. Ramu, T. Srinivasan, G. Suresh, C.M. Meenakshi, R. Lavanya, Static investigation of Roselle waste powder reinforced bio polymer composite. J. Phys. Conf. Ser. **2054**(1), 012058 (2021)
38. E. Muñoz, J.A. García-Manrique, Water absorption behaviour and its effect on the mechanical properties of flax fibre reinforced bioepoxy composites. Int. J. Polym. Sci. **2015**, 390275 (2015)
39. S. Banerjee, B.V. Sankar, Mechanical properties of hybrid composites using finite element method based micromechanics. Compos. Part B-Eng. **58**, 318–327 (2014)
40. M.R. Bowditch, The durability of adhesive joints in the presence of water. Int. J. Adhes. Adhes. **16**(2), 73–79 (1996)
41. M.A. Ghafaar, A.A. Mazen, N.A. El-Mahallawy, Application of the rule of mixtures and Halpin–Tsai equations to woven fabric reinforced epoxy composites. J. Eng. Sci. **34**(1), 227–236 (2006)
42. A.G. Facca, M.T. Kortschot, N. Yan, Predicting the elastic modulus of natural fibre reinforced thermoplastics. Compos. Part A-Appl. S. **37**(10), 1660–1671 (2006)
43. I. Van de Weyenberg, T. Chi Truong, B. Vangrimde, I. Verpoest, Improving the properties of UD flax fibre reinforced composites by applying an alkaline fibre treatment. Compos. Part A-Appl. S. **37**(9), 1368–1376 (2006)
44. M. Aly, M.S.J. Hashmi, A.G. Olabi, K.Y. Benyounis, M. Messeiry, A.I. Hussain, E.F. Abadir, Optimization of alkaline treatment conditions of flax fiber using Box–Behnken method. J. Nat. Fibers **9**(4), 256–276 (2012)
45. W. Frącz, G.L. Janowski, Bąk influence of the alkali treatment of flax and hemp fibers on the properties of PHBV based biocomposites. Polymers **13**, 1965 (2021)
46. M. Hosur, H. Maroju, S. Jeelani, Comparison of effects of alkali treatment on flax fibre reinforced polyester and polyester-biopolymer blend resins. Polym. Polym. Compos. **23**(4), 229–242 (2015)
47. H. Zhang, R. Ming, G. Yang, Y. Li, Q. Li, H. Shao, Influence of alkali treatment on flax fiber for use as reinforcements in polylactide stereocomplex composites. Polym. Eng. Sci. **55**(11), 2553–2558 (2015)
48. S. Chokshi, V. Chaudhary, P. Gohil, Tensile properties prediction of unidirectional flax/polyester composites: mathematical modeling and experimental investigation. Fibers Polym. **23**(10), 2945–2951 (2022)
49. S. Chokshi, P. Gohil, Experimental investigation and mathematical modeling of longitudinally placed natural fiber reinforced polymeric composites including interphase volume fraction. Fibers Polym. **23**(2), 488–501 (2022)